

Irregular diffusion in the bouncing ball billiard

L. Matyas and R. Klages

Max Planck Institute for the Physics of Complex Systems,
Nothnitzer 38, 01187 Dresden, Germany

Abstract

We call a system bouncing ball billiard if it consists of a particle that is subject to a constant vertical force and bounces inelastically on a one-dimensional vibrating periodically corrugated floor. Here we choose circular scatterers that are very shallow, hence this billiard is a deterministic diffusive version of the well-known bouncing ball problem on a flat vibrating plate. Computer simulations show that the diffusion coefficient of this system is a highly irregular function of the vibration frequency exhibiting pronounced maxima whenever there are resonances between the vibration frequency and the average time of flight of a particle. In addition, there exist irregularities on smaller scales that are due to higher-order dynamical correlations pointing towards a fractal structure of this curve. We analyze the diffusive dynamics by classifying the attracting sets and by working out a simple random walk approximation for diffusion, which is systematically refined by using a Green-Kubo formula.

Key words: fractal diffusion coefficient, bouncing ball, granular material, phase locking

PACS: 47.20.Ky, 46.40.Ff, 47.53.+n, 45.70.-n

1 Introduction

An important challenge in the field of nonequilibrium statistical mechanics is to achieve a more profound understanding of transport processes by starting from the complete microscopic, deterministic, typically chaotic equations of motion of a many-particle system [1-3]. However, up to now such a detailed analysis concerning the microscopic origin of nonequilibrium transport could only be performed for certain classes of toy models. Very popular among these models are systems that are low-dimensional, spatially periodic and consist of a gas of moving point particles that do not interact with each other but only with fixed scatterers.

For these chaotic dynamical systems it was found that, typically, the respective transport coefficients are highly irregular functions of the control parameter. These irregularities were exactly calculated for diffusion in a simple abstract piecewise linear map [4,6] and were shown to be related to topological instabilities under parameter variation. The same properties are exhibited by dissipative Hamiltonian particle billiards such as the periodic Lorentz gas [7,8], the flower-shaped billiard [9], and for a particle moving on a one-dimensional periodically corrugated floor [10]. Similar irregularities occur in nonhyperbolic maps with anomalous diffusion [11] in simple models exhibiting (electric) currents [12,13] as well as in the parameter dependence of chemical reaction rates in reaction-diffusion processes [14]. In most of the cases mentioned above, the deterministic transport coefficients clearly showed fractal structures [4,6,8,10,12,14]. Seemingly analogous transport anomalies were measured in experiments [15,16] or have been reported for models that appear to be rather close to experiments [17,18]. However, still an experimental verification of the fractal nature of irregular transport coefficients remains an open question.

In this paper we wish to contribute to this problem by introducing and investigating a dynamical system that, we believe, is rather close to specific experiments. For this purpose we consider a generalized version of the interesting model described in Ref. [10], where a particle subject to a constant vertical acceleration makes jumps on a periodically corrugated floor. We generalize this model by including some friction at the collisions and compensate this energy loss by periodic oscillations of the corrugated floor. This generalized model is an example of what we call a bouncing ball billiard. It is designed to be very close to the experiments on diffusion in granular material performed in Refs. [19,21], thus we hope that our theoretical predictions can be verified by respective experiments. However, we emphasize the fact that, in contrast to most experiments on granular material,¹ here we study a granular gas that consists of statistical ensembles of a one-particle system only. One should therefore be very careful in concluding anything from the physics we discuss here for the case of highly interacting many-particle systems.

The corrugated floor of our model is formed by circular scatterers that are deliberately very shallow. Hence, another important limiting case of our model is the famous bouncing ball problem, where an inelastic particle bounces vertically on a flat vibrating surface. This problem has both been studied experimentally [22,26] as well as theoretically [27,30]. It is well-known that the nonlinear dynamics of the bouncing ball is very complex exhibiting one or more coexisting attractors depending on the frequency of the floor [31], that is, the system displays both ergodic and nonergodic dynamics. The main theme of this paper will be to show that dynamical correlations in terms of phase locking, as

¹ An exception is the experiment performed in Ref. [19] where the dynamics is exclusively due to the collisions of a single particle with a corrugated surface.

associated to these different attractors, have a huge impact on diffusion in the bouncing ball billiard and that these regimes lead to strong irregularities in the parameter-dependent diffusion coefficient on large and small scales.

The paper is composed of six sections: In Section 2 we outline some important features of the bouncing ball problem. This knowledge provides a roadmap in order to understand the diffusive behavior in the spatially extended system. In Section 3 we give the full equations of motion of the bouncing ball billiard and briefly explain the specific choice of the control parameters. In Section 4 we present results for the diffusion coefficient and for the average energy of the system as functions of the frequency of the vibrating floor. In Section 5 we analyze the irregularities of the parameter-dependent diffusion coefficient in full detail by relating them to different dynamical regimes, as represented by certain structures in the corresponding attracting sets. In Section 6 we work out a simple random walk approximation somewhat explaining features of the diffusion coefficient on the coarsest scales. This approach is then refined by including higher-order dynamical correlations based on a Green-Kubo formula for diffusion thus providing detailed evidence for the existence of irregularities on finer and finer scales. Section 7 contains a summary of the results, an outline of further links to previous works, and an outlook concerning further studies in this direction. In particular, we are trying to encourage an experimental realization of our bouncing ball billiard.

2 The bouncing ball problem : A mold tongues

A standard problem of chaotic dynamics that was extensively studied is the one of a ball subject to an external field that bounces inelastically on a flat vibrating surface [26,30,32]. At first view this model appears to be rather simple, however, its equations of motion are in fact highly nonlinear and generally do not allow any exact solution. Hence, a good part of the investigations deals with simplified versions of this model such as the so-called high bounce approximation leading to the dissipative standard map [26,31]. Here we restrict to the exact model only as nicely analyzed in Refs. [26,30] and recall some important features that will be needed to understand the forthcoming results.

Let us assume that the flat surface exhibits a sinusoidal motion $y = A \sin(\omega t)$, where A and ω are the amplitude respectively the frequency of the vibration. Between the bounces on the surface the ball moves in a gravitational field with acceleration g . If the mass of the ground plate is assumed to be much larger than the mass of the ball, the latter becomes a trivial quantity in the equations of motion that, for convenience, we set equal to one. The bouncing ball problem then has four control parameters: A , ω , the gravitational acceleration g and the vertical restitution coefficient ϵ . After a proper transformation of

the equations of motion $\ddot{A}, \dot{!}$ and g can be grouped into $\ddot{A} + \omega^2 A = g$. A particular complexity of the bouncing ball system is related to the fact that for given values of the parameters ω and g the system may possess more than one attractor, each with a different basin of attraction. This is drastically exemplified in a study of the high-bounce approximation revealing the coexistence of an arbitrarily large number of attractors if the damping is small enough [31].

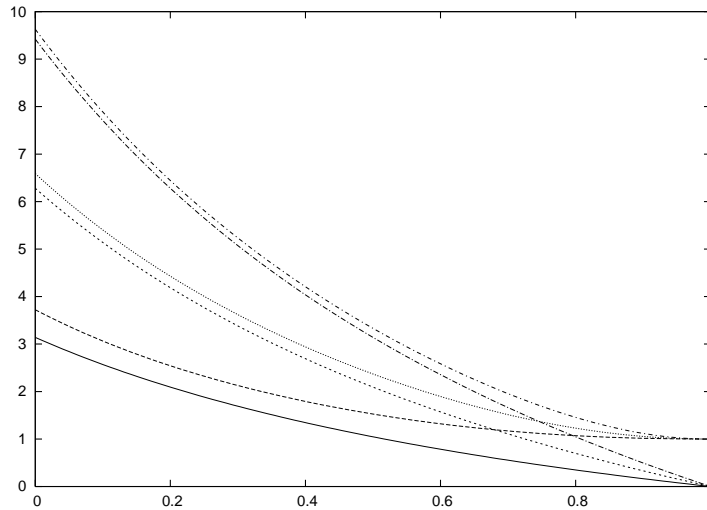


Fig. 1. The three main Arnold tongues of the bouncing ball problem in parameter space. The adjacent odd and even lines represent the boundaries of the resonances between the period of the driving T_{vibr} and the time of flight between two bounces T_{ight} , see Eq. (1). From bottom to top it is $T_{ight} = T_{vibr} = 1; 2; 3$. ω and g are dimensionless quantities.

We will now focus on the Arnold tongues of the bouncing ball defining a series of stable resonances. The largest ones were analyzed approximately in Refs. [23,25] and were later on calculated exactly in Ref. [30]. An account of the hierarchy of smaller ones in the limit of zero friction was approximately given in Ref. [29]. A resonance of order $k=1$ means that the period of the particle's flight between two collisions T_{ight} is k times larger than the period of the driver's motion, $T_{ight} = k T_{vibr}$, $k \in \mathbb{N}$. The region in parameter space $(\omega; g)$ where a resonance of order k exists can then be calculated via linear stability analysis of the equations of motion to [30]

$$\frac{1}{1+k} < \omega < \frac{1}{1+k} + \frac{2(1+k^2)^{\frac{1}{2}}}{(1+k)^2}; \quad g < \frac{2(1+k^2)^{\frac{1}{2}}}{(1+k)^2} \quad (1)$$

These different Arnold tongues are shown in Fig. 1. Note that, somewhat in contrast to simple Arnold tongues, here not all the initial conditions in phase space may exhibit phase locking. That is, typically there are in addition nonresonant trajectories that will "stick" to the surface interrupted by sequences in which they are relaunched exhibiting jumps of smaller and smaller amplitude. This

particularly complicated dynamics was denoted as "self-reanimating chaos" [25] or as "chattering" [30]. In Ref. [30], a careful analysis indeed led to the result "that generic trajectories starting under experimental conditions terminate in a region of chattering", which seemed to be at variance with the experimental observation of a Feigenbaum-like bifurcation scenario and a respective transition to chaos [22,26].

3 The bouncing ball billiard

3.1 Equations of motion and control parameters of the model

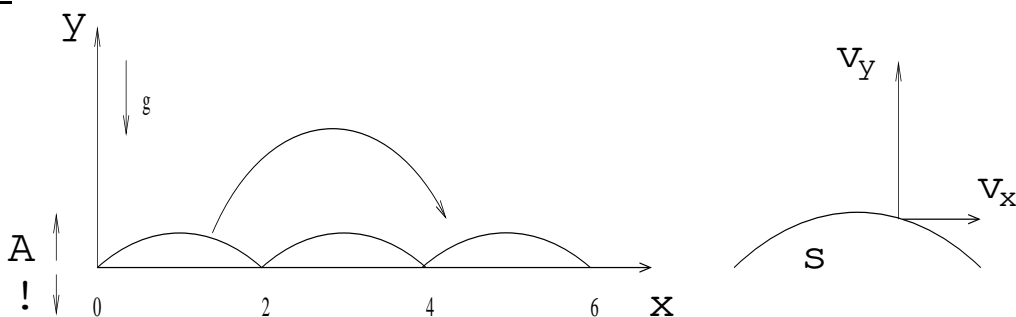


Fig. 2. Illustration of the bouncing ball billiard studied here: A moving point particle is colliding inelastically with circular scatterers that are periodically distributed on a line. Parallel to y there acts an external field with constant acceleration g . The floor of scatterers oscillates with an amplitude A and a frequency $!$.

The bouncing ball billiard that we study in this paper, with the floor formed by circular scatterers, is depicted in Fig. 2.

The equations of motion of this system are defined as follows: The particle performs a free flight in the gravitational field g k y between two collisions. Correspondingly, its coordinates $(x_{n+1}; y_{n+1})$ and velocities $(v_{x,n+1}; v_{y,n+1})$ at time t_{n+1} immediately before the $n+1$ th collision and its coordinates $(x_n^+; y_n^+)$ and velocities $(v_{x,n}^+; v_{y,n}^+)$ at time t_n immediately after the n th collision are related by the equations

$$x_{n+1} = x_n^+ + v_{x,n}^+ (t_{n+1} - t_n) \quad (2)$$

$$y_{n+1} = y_n^+ + v_{y,n}^+ (t_{n+1} - t_n) - g (t_{n+1} - t_n)^2 = 2; \quad (3)$$

$$v_{x;n+1} = v_{x,n}^+ \quad (4)$$

$$v_{y;n+1} = v_{y,n}^+ - g (t_{n+1} - t_n) : \quad (5)$$

At the collisions the change of the velocities is given by

$$v_{zn}^+ - v_{ci?n} = (v_{ci?n} - v_{zn}) \quad (6)$$

$$v_{kn}^+ - v_{cikn} = (v_{kn} - v_{cikn}) ; \quad (7)$$

where v_{ci} is the velocity of the corrugated floor. Here we distinguish between the different velocity components relative to the normal vector at the surface of the scatterers, where the scatterers are represented by the arcs of the circles forming the floor. v_z , v_k and $v_{ci?}$, v_{cik} indicate the normal, respectively tangential components of the particles, respectively the floor's velocity with respect to the surface at the scattering point. Correspondingly, we introduce two different restitution coefficients e_n and e_{cn} that are perpendicular, respectively tangential to the normal.

As in case of the standard bouncing ball problem we assume that the floor oscillates sinusoidally, $y_{ci} = A \sin(\omega t)$, where A and ω are the amplitude respectively the frequency of the vibration, see Fig 2. Hence, the phase space is defined by the variables $(t; x; y; v_x; v_y)$, where the time variable needs to be included because we have a driven system described by nonautonomous differential equations. If we record only the collision events with the floor, as it is usually done in case of the bouncing ball, the dimension of the phase space can be reduced accordingly. For this purpose we use the position of the collision at the circumference of a scatterer defined by the clockwise arclength at the impacts and the horizontal and vertical velocities just after a collision, $z = (s; v_x^+; v_y^+)$. In such a Poincare section the time-continuous flow is equivalent to the time-discrete map

$$\begin{aligned} z_{n+1} &= f(z_n) \\ t_{n+1} &= t_n + \tau(z_n) \\ l_{n+1} &= l_n + a(z_n) : \end{aligned} \quad (8)$$

called a suspended flow in Refs. [1,10,33]. In the second equation $\tau(z)$ is the time of flight between two successive collisions, and in the third equation $a(z_n)$ counts the number of scatterers, or tiles, the particle has jumped over during a flight, l_n being the tile where the particle has actually started at the n th collision, hence l_n is an integer. If the billiard is simple enough, these equations can be derived analytically, such as in case of the periodic Lorentz gas [1,33] and in case of the completely elastic non-vibrating floor [10]. This enormously simplifies the computer simulations since the mapping has merely to be iterated numerically. However, in case of the bouncing ball billiard due to the vibrations we were not able to derive the exact form of this mapping. Hence, the equations of motion were solved via discretizing the parabolic flight between collisions in time and trying to accurately determine the point of the collision with the surface by reducing the time lag of the iterations to 10^{-6} s at collision events.

3.2 Choosing the parameters of the billiard

We choose the parameters of the billiard in Fig. 2 according to a possible experimental setup [21]. The extension of each scatterer we determine to $d = 2\text{ mm}$. In our study we fix the value of ω and increase the value of Ω . This can be done by tuning the frequency $f = \Omega/2\pi$ while keeping the amplitude constant at $A = 0.1\text{ mm}$. The gravitational acceleration is taken to be $g = 9.8\text{ m/s}^2$. The value of the normal restitution coefficient is chosen to $\epsilon = 0.5$ such that the major resonances as depicted in Fig. 1 do not overlap with each other. Since our model has the geometry of a dispersing billiard, the arcs induce a dynamical instability that somewhat counteracts the stability in presence of a resonance. More importantly, the arcs make the system dissipative by feeding energy that is vertically pumped into the system also into the respective x -component of the velocity.

The main purpose of our model is to study the impact of dynamical correlations on the deterministic diffusion coefficient, hence we would like to preserve the mechanism related to the resonances of the bouncing ball problem as much as possible.² Consequently, the radius of the scatterers should be very large. Here we choose the radius R of the arcs and the corresponding curvature to $K = 1/R = 0.04\text{ mm}^{-1}$. Note that, because of the spatial periodicity, this billiard is of the form of a two-particle problem with periodic boundary conditions. Since the radii of the scatterer and of the particle are simply additive, a periodic surface with respective radii could be realized experimentally by choosing a suitably large radius of the moving particle (which, of course, may have other side effects on which we do not elaborate here).

At parameter values where no resonance is possible the particle may "stick" to the surface for some time, that is, it will land at a certain position and, because of the friction, it will be relaunched at the next period of the oscillation. However, in case of fully elastic tangential scattering with $\epsilon = 1$, because of the spatial extension long trajectories may occur at which a particle "slides" along the surface in one direction even if its vertical velocity relative to the surface of the scatterer is zero. In order to avoid these rather unphysical horizontal slides, we set the value of ϵ smaller than one. Numerically it turned out that

² We briefly remark that, by starting from the curved surface of Ref. [10] and making the originally Hamiltonian dynamics dissipative, first simulations seemed to indicate that the irregular structure of the diffusion coefficient was rather immediately destroyed. That may be related to the fact that certain periodic orbits associated to small islands of stability, which indirectly determined this structure, are straightforwardly eliminated by inclusion of dissipation. Furthermore, the oscillations of the plate profoundly disturbed the original Hamiltonian dynamics. The precise nature of the transition between the Hamiltonian case and the dissipative case may be an interesting problem for further studies.

a horizontal restitution of $\epsilon = 0.99$ is already sufficient to eliminate all slides. We remark that this value is still considerably larger than the ones found in experiments on inelastic particle collisions [34], however, with the choice of this value we avoid the vanishing of the diffusion coefficient at certain values of the frequency.

Instead of using the dimensionless parameter ϵ we make our following presentations in terms of the frequency f , since with a variation in steps of 0.2Hz it affects $\epsilon = A/4f^2 = g$ only in the third digit after the comma, consequently the frequency provides a much better scale. This translates the position of the Arnold tongues in the bouncing ball problem at $\epsilon = 0.5$, as shown in Fig. 1, as follows: 1=1-resonance: $f \in [50.98; 61.56]\text{Hz}$; 2=1-resonance: $[72.10; 76.71]\text{Hz}$; 3=1-resonance: $[88.30; 90.95]\text{Hz}$. The position of the tongues is also indicated in Fig. 3. In the following, the diffusion coefficient is presented in units of mm^2/s and the energy in kgmm^2/s^2 .

4 The frequency-dependent diffusion coefficient of the bouncing ball billiard

If we choose the set of parameters as explained in Sec. 3.2, we expect that the dynamics of the spatially extended system is to a large extent somewhat determined by the one of the bouncing ball problem. However, as was outlined in Sec. 2, for the bouncing ball problem time and ensemble averages often strongly depend on the initial conditions, i.e., the system is nonergodic. In the bouncing ball billiard this deficiency is eliminated by the defocusing character of the scatterers, i.e., the dynamics is getting ergodic, except for some short frequency intervals at small frequencies around the 1=1-resonance. That is, the dynamics typically evolves on only one or sometimes on two attractors. The details related to these phase space properties will be worked out in Sec. 5. Here we focus on the coarse structure of the diffusion coefficient as related to regions of resonances.

For any frequency located in the interval of $f \in [49.77; 95.0]\text{Hz}$ the system was found to evolve into a nonequilibrium steady state. This was checked in terms of the average (kinetic, total) energy of the moving particle, which was always approaching a constant value for large times. The diffusion coefficient in the horizontal direction was then obtained from the Einstein formula

$$D = \lim_{t \rightarrow \infty} \frac{\langle (x(t) - x(0))^2 \rangle}{2t}; \quad (9)$$

where the brackets denote an ensemble average over moving particles. The diffusion coefficient was converging to a specific value for large enough times.

The size of the ensemble of points consisted of 10^3 initial conditions that uniformly filled the phase space region of $0 \leq x \leq 2.0004\text{m}$, $v_x^+ \leq v_x \leq -40\text{m/s}$, and $0 < v_y^+ \leq v_y \leq 40\text{m/s}$.³

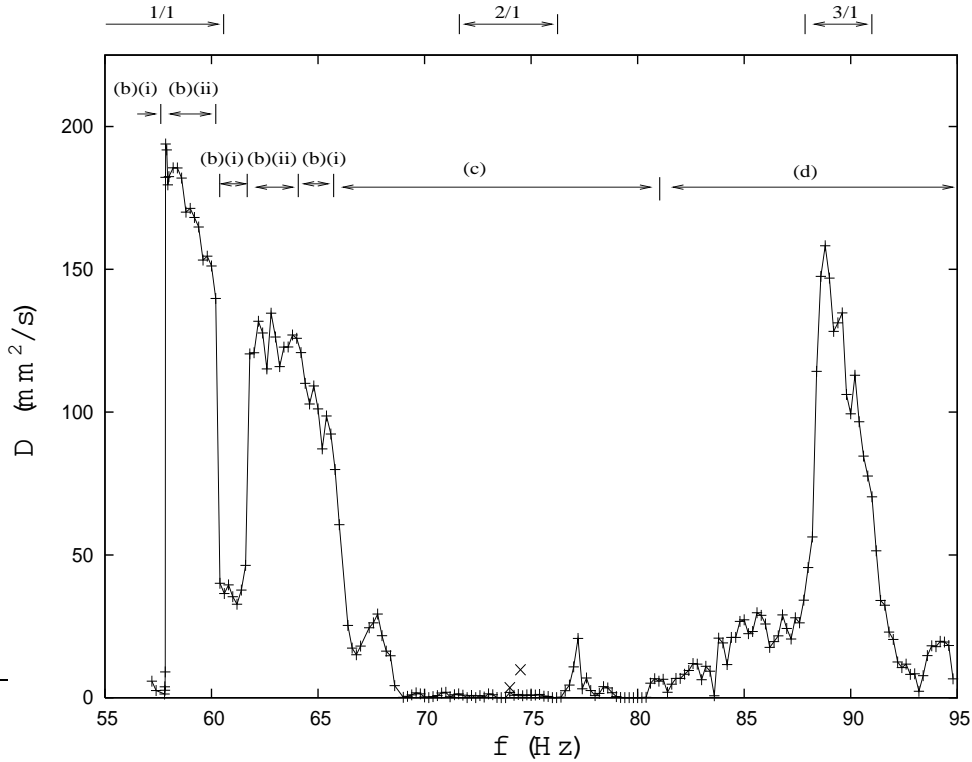


Fig. 3. The diffusion coefficient of the bouncing ball billiard as a function of the vibration frequency of the corrugated floor. The frequency range of the non-diffusive bouncing ball resonances, see Fig. 1 at $\alpha = 0.5$, are shown on top of the frame. They suggest a strong impact of the resonances on the diffusion coefficient. However, the fine structure of this curve appears to be more complex than merely explained by the resonances. Different dynamical regimes, as thoroughly discussed in Sec. 5, are indicated in this figure in form of horizontal arrows. The two crosses (x) at the frequencies 74.0 Hz and 74.5 Hz reveal the existence of the second resonance but were only obtained by sampling a larger set of initial conditions. The standard deviation errors are smaller than the magnitude of the symbols.

³ For a considerable number of frequency values the results for the diffusion coefficient have been cross-checked by sampling the initial conditions for the ensemble from one long trajectory. That is, we take as initial conditions coordinates from this trajectory after the dynamics has evolved a random fraction of a maximum time that is considerably larger than the time of typical transients. Within errorbars, the same results have been obtained for the diffusion coefficient. However, this cross-check could not easily be performed for frequency intervals marked by (b)(i) in Fig. 3 where the dynamics is nonergodic. In these cases the ensemble was still the one described in Sec. 4, apart from the two points indicated in Fig. 3, and the results may thus depend on the choice of initial conditions if other attracting sets were not sampled by the specific set of initial conditions.

The dependence of the diffusion coefficient on the frequency is depicted in Fig.3. This figure clearly demonstrates that whenever the value of the frequency reaches the different major A mold tongues as discussed in Sec.2, the diffusion coefficient has considerably larger values than elsewhere and consequently exhibits local maxima.

Above the frequency regime corresponding to the $l=1$ A mold tongue, that is, for $f > 70$ Hz, the diffusion coefficient becomes very small but is still different from zero in that it has a value around one or two. This phenomenon lasts until $f < 80$ Hz. Note that for a smaller tangential restitution coefficient this region would collapse to $D = 0$ m²/s. Fig.3 shows that at the frequencies associated to the $l=1$ and to the $3=1$ resonances the diffusion coefficient is about two orders of magnitude larger than the ones at $f \in [70;80]$ Hz.

Irrespective of the specific frequency value, after a transient time the average of the total energy converges to a constant value indicating the existence of a nonequilibrium steady state. These values are presented in Fig.4 as a function of the frequency. This curve resembles very much the parameter-dependent diffusion coefficient. However, as may be expected intuitively the value of the diffusion coefficient is even more closely associated with the average kinetic energy related to the horizontal velocity component $v_x^2=2$, see Fig.5. Still, in detail the structure of the diffusion coefficient cannot be trivially understood on the basis of the frequency dependence of the (kinetic) energy only, or vice versa; see Sec. 6 for further details. It is also interesting to note here that there is no equipartitioning of energy between the x and the y coordinate. Fig. 4 furthermore includes a lower bound for the energy of a moving particle, which presents the case when it sticks to the surface and behaves like a simple harmonic oscillator. This approximation indicates an increase of the total energy, and of the corresponding horizontal kinetic energy, on a large scale which, however, appears to be largely obscured by the superimposed oscillations of the energy.

A further interesting feature of these three figures is that above $f > 80$ Hz particularly the diffusion coefficient, and to some extent also the average energies, seem to experience a pronounced average increase on larger scales. This property somewhat reminds of the phase transition-like behavior discussed in Ref. [19] where the average horizontal velocity of a granular multilayer of particles in an asymmetric periodic potential shows a sudden growth from zero to a nonzero value.

Finally, we would like to draw the attention to a particularly interesting detail of these curves: Around $f < 60$ Hz in the first resonance there appears to be an almost perfect linear decrease of the average total energy, and correspondingly of the associated kinetic energy, whereas just in the same region the diffusion coefficient exhibits some rather regular oscillations on fine scales. One may

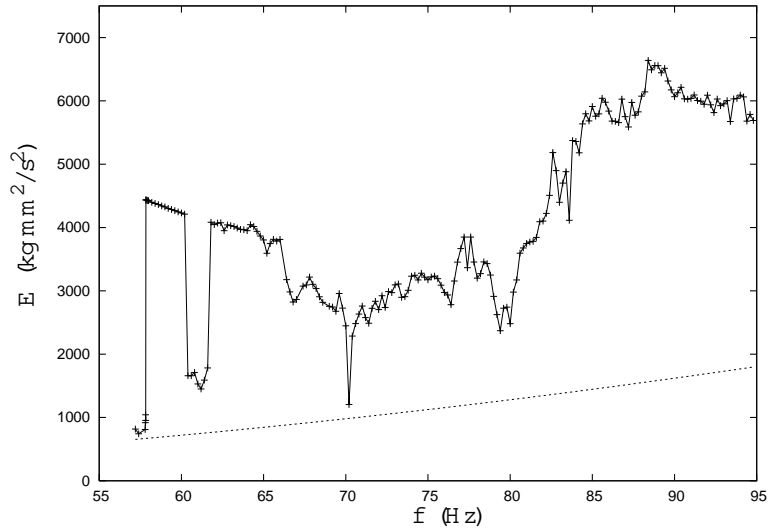


Fig. 4. The average total energy as a function of the vibration frequency. The dotted line shows the possible minimal energy a particle can have, which is the energy of a harmonic oscillator sticking to the surface, $A^2 \omega^2 = 2$.

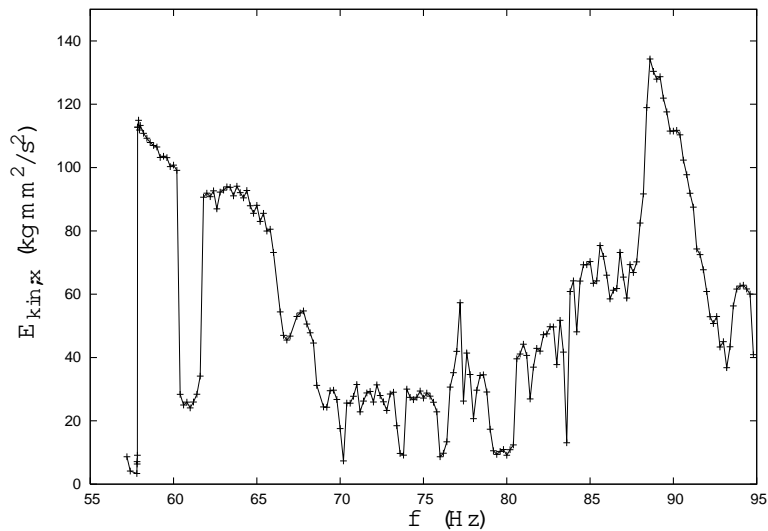


Fig. 5. The average horizontal kinetic energy, that is, $E_{kin,x} = v_x^2 = 2$, as a function of the vibration frequency. One can see that the structure of the kinetic energy closely follows the one of the diffusion coefficient in Fig. 3.

argue that here the variation of the energy, as a function of the frequency, provides a linear "ramp" that essentially reduces the bouncing ball billiard to the system of Ref. [10], where the diffusion coefficient was studied as a function of the energy as a control parameter. Indeed, the diffusion coefficient of Ref. [10] too exhibited some very regular, apparently fractal oscillations under variation of the energy, which qualitatively very much resemble the ones that appear in the respective small region of Fig. 3. We will get back to a more refined analysis of the fine structure of the whole curve in Sect. 6.

5 The different dynamical regimes of the bouncing ball billiard

Depending on the driving parameter ϵ , or respectively on the frequency f , the following dynamical regimes can be distinguished in the bouncing ball billiard:

(a) When $\epsilon < 1$ the maximal acceleration of the floor is smaller than the gravitational force, $A!^2 < g$, consequently once the particle lands on the surface it will never leave it again. In this case the particle is eventually located in one of the wedges that the arcs of two adjacent circles form with each other. Hence, after a short transient period the particle will be in phase with the surface and its relative velocity to the floor will be zero. For our parameters this happens up to the frequency $f_0 = 49.77\text{ Hz}$. For frequency values just above f_0 a particle can be relaunched from the floor, however, because of the inelasticity of the collisions and due to the height of the arcs typically the particle remains trapped in the wedges of the billiard. Numerically we find that around $f = 57\text{ Hz}$ particles start to leave a wedge for the first time, as shown in Fig. 3, consequently we consider this value as the onset of diffusion, despite the drastic increase that takes place right afterwards around $f = 58\text{ Hz}$.

(b) The most interesting dynamical regime appears to be associated with the $1=1$ -resonance of the bouncing ball. In case of a flat vibrating plate there are two attractors at these frequencies, one showing this resonant behavior and another one with particles that stick to the surface. In case of the bouncing ball billiard this dynamical regime exhibits a complex scenario under variation of the frequency, where due to the convexity of the scatterers also ergodic motion becomes possible. This suggests to distinguish between two different types of dynamics: (i) There are frequency regions where the system has two coexisting attractors, one representing the $1=1$ -resonance, and a second one showing an intermittent-like behavior consisting of long periods of stick and slip, or "creepy" motion. This nonergodic regime is located at the frequency intervals $f \in [57.0; 57.8]\text{ Hz}$, $f \in [60.4; 61.8]\text{ Hz}$ and $f \in [63.4; 65.6]\text{ Hz}$, see Fig. 3. (ii) The other type of behavior is represented by frequencies at which there is only one attractor with all initial conditions leading to the same phase locking. These frequency intervals are at $f \in [58.0; 60.2]\text{ Hz}$ and at $f \in [62.0; 63.2]\text{ Hz}$. It is remarkable that whenever particles are in resonance with the plate the motion becomes regular only in the vertical direction. In this direction we then have a $1=1$ phase locked dynamics similar to the respective resonance of the bouncing ball. However, in the horizontal direction we still find a highly irregular behavior as quantified by the diffusion coefficient. In order to illustrate this dynamics we look at a projection of the phase space at the collisions of a particle with the floor. Because of the resonance the vertical velocity has approximately the same value at the collision such that we almost have a Poincaré section of the dynamics. Thus we only consider the positions of the colliding particle on the circumference of a scatterer and the horizontal

velocity v_x right after a collision, see Fig. 6.

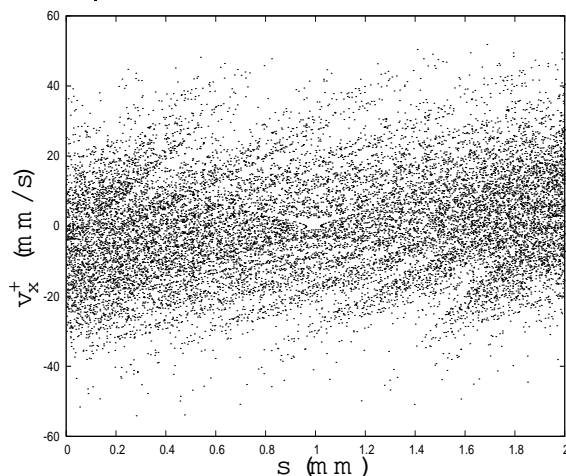


Fig. 6. Projection of the phase space in the $l=1$ resonance where the vertical dynamics is approximately in phase with the vibration frequency, which is here $f = 58\text{Hz}$. s marks the clockwise position of the colliding particle at the circumference of a scatterer and v_x^+ denotes the horizontal velocity right after a collision.

In this figure one can detect traces of a separatrix structure around the unstable fixed point at $s = 1; v_x^+ = 0$ corresponding to the two cases where a particle can leave a wedge, i.e., the trajectory goes over $s = 1$, or it cannot, i.e., the particle does not approach the peak of an obstacle or simply turns back in the neighbourhood of $s = 1$. In addition, there are interesting parts of the phase space outside the separatrix in the regions of $s < 1, v_x^+ > 0$, respectively $s > 1, v_x^+ < 0$. Here particles go "uphill" by generating a fan-shaped structure in phase space showing that specific paths are chosen according to which particles are allowed to leave a wedge, whereas other possibilities are apparently forbidden. Yet there is no evidence that particles creep along the surface of a scatterer in form of long sequences of very tiny hops, cp. to Fig. 7, however, one may speculate that the fan-shaped structure presents a precursor of such creeps. We furthermore remark that for this figure the dynamics is ergodic and that the average energy of a particle saturates after several hundred collisions such that we get a good convergence at this frequency.

(c) Between the frequencies $f = 65.8\text{Hz}$ and $f = 81.0\text{Hz}$ the dynamics is characterized by long creeps. Consequently, leaving the wedges takes a long time and suppresses diffusion. In the neighbourhood of the frequency 74Hz the $2=1$ -resonance could be detected, however, this resonance could only be revealed by choosing a set of initial conditions that is considerably more extended over the phase space than at the other frequencies, with initial conditions of $v_y^+ > 100\text{m/s}$. The results indicated by the two specially marked points in Fig. 3 at the frequencies 74Hz and 74.5Hz show that the impact of this resonance on the diffusion coefficient is, according to the respective measure of such orbits in the nonergodic phase space, rather small. Note that, apart from this

special case, we had no indication for other non-ergodic behavior in regime (c).

We furthermore note the existence of another small peak around 77 Hz that is still close to the region of this resonance. Curiously, the following simple reasoning precisely identifies this frequency as a special point of the dynamics: Let us assume that a particle behaves similar to a harmonic oscillator sticking to the surface. Then, as argued above, its average vertical kinetic energy is equal to $E_y = A^2 \omega^2 / 2$. However, for diffusion this energy should be large enough such that a particle can pass an obstacle, which is here of the height $h = 0.02 \text{ mm}$. Consequently, if the particle acquires a potential energy that is equal to $E_{\text{pot}} = g(A + h)$ it can pass any scatterer even at the highest position of the vibrating plate. Of course, in this simple reasoning we have disregarded any impact of the two restitution coefficients as well as the fact that, additionally, some horizontal kinetic energy is necessary in order to perform a diffusion process. In any case, a respective calculation yields $f = 77.23 \text{ Hz}$ precisely corresponding to the position of this small peak. One may furthermore speculate that this argument is somewhat related to the onset of the global increase of the diffusion coefficient and of the energy as discussed in Sec. 4.

(d) For the next, in this study the last dynamical regime with $f \in [81.1; 95.0] \text{ Hz}$ Figs. 4 and 5 demonstrate a noticeable increase of the average total and horizontal kinetic energies that appears to be reflected in a respective increase of the diffusion coefficient on a coarse scale. Now the particle spends considerably more time moving around than sticking to the surface. Indeed, we find that the dynamics is ergodic such that, in contrast to region (b), here both types of resonant and creeping motion are intimately linked to each other, instead of appearing in coexisting attractors, or at different frequencies. This type of dynamics is represented by the attractor of Fig. 7, where the coordinates s and v_x are shown at the frequency $f = 85.2 \text{ Hz}$.

In spite of the fact that particles creep from time to time along the surface,⁴ as we can clearly see in the attractor of Fig. 7, the average energy of a particle launched from randomly chosen initial conditions on this attractor saturates. Consequently, a system of noninteracting particles reaches a nonequilibrium steady state in this regime, too.

At the frequency interval of the $3=1$ resonance one can now find a quasi-locked orbit, see Fig. 8, that still induces a strong maximum in the diffusion coefficient. At first view this orbit indeed appears to resemble a period 3 orbit, however, closer inspection of the y coordinate reveals that it may rather have bifurcated into portions that resemble an orbit of period 6. The right half of Fig. 8 depicts these six regions that are visited one after the other. However, an even closer

⁴ For the probability and the respective fraction of time of sticking to the surface see [30,32].

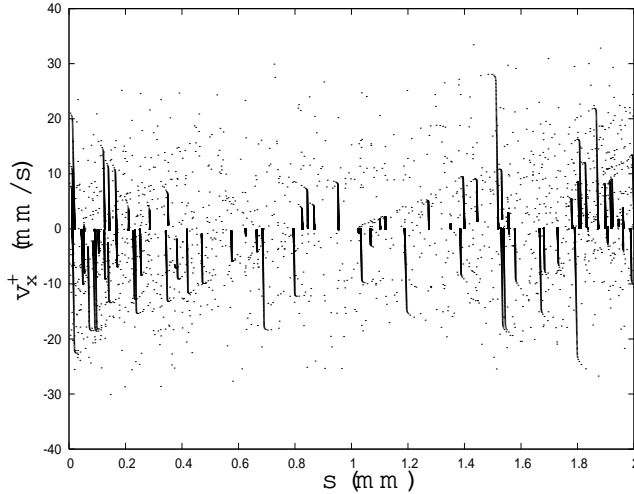


Fig. 7. Projection of the phase space at the frequency of $f = 85.2\text{Hz}$ representing a dynamical regime where particles "creep" along the surface. These creeps are visible in form of the almost vertical lines indicating that a particle performs long sequences of correlated jumps nearly at the same position with smaller and smaller horizontal velocities. The coordinates are the same as in Fig. 6.

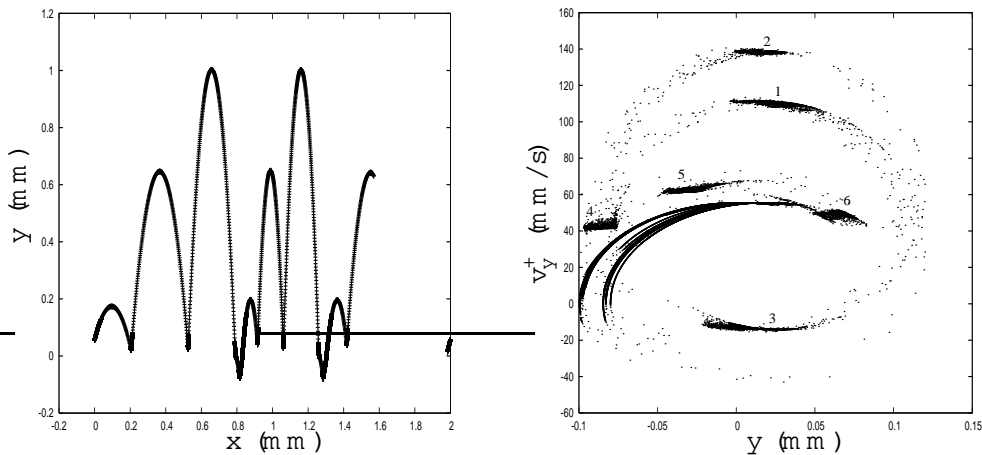


Fig. 8. A sequence of a particle's trajectory at $f = 88.4\text{Hz}$ (left) and the corresponding attractor in the plane $(y; v_y^+)$ (right). These figures show the deformation of the previous $3=1$ -resonance into a much more complicated quasi-periodic orbit.

look reveals that in fact this is a period 11 orbit: the trajectory first follows the positions 1 to 6, but at any second sequence it skips the position 6 and goes instead directly from position 5 to the position 1. Even more, sometimes the particle misses the last landing at position 4 and gets stuck at the surface. It is then relaunched at the next period, with the next bounce after the relaunch at position 5, and the periodic orbit starts again.

In summary, for all frequencies there appear to exist essentially four different types of dynamical regimes: if the diffusion coefficient is very large, the dynamics typically exhibits some type of periodicity that is responsible for

an enhancement of diffusion. Either this dynamics is strictly associated to an original bouncing ball resonance, as in case of the regimes (b) (ii), or the resonance still appears in a deformed way as in case of the largest peak in region (d). If the diffusion coefficient is getting smaller there is an intermediate regime in which two different attractors with resonances and creeping motion coexist, and the dynamics is non-ergodic, see regimes (b) (i) and the small peak around $f = 74\text{Hz}$. However, it is also possible that the motion in this intermediate regime is intermittent-like and ergodic, by alternating between localized creeps and long flights. Finally, if the diffusion coefficient is getting closer to zero, there is typically only sticky motion as discussed for region (c). Fig. 6 exemplifies the regime of large diffusion coefficients, whereas Fig. 7 shows portions of typical creeping dynamics. Note that, since we do not know about the position of any higher-order Arnold tongues in the phase diagram Fig. 1, we cannot possibly associate smaller peaks in the diffusion coefficient to such higher-order tongues, but we cannot exclude that this is possible. In any case, in the next section we outline a simple approach that helps to explain the origin of the structure of the diffusion coefficient particularly on smaller scales.

6 The fine scale of the coefficient: correlated random walk approximations

As we explained in the previous section, the huge peaks in the diffusion coefficient are associated with the major resonances of the bouncing ball problem. However, first of all we have not yet clarified what large scale functional dependence one would expect for the diffusion coefficient based on stochastic theory. In addition, one observes a lot of irregularities on finer scales in Fig. 3 whose origin needs to be commented upon. In this section we work out some simple random walk arguments as well as systematic refinements of it, which were called correlated random walk approximations [8], in order to achieve a more detailed understanding of Fig. 3.

We first start with a simple approximation that is based on the picture of diffusion as a random walk on the line. Let us assume that the wedges of the billiard act as "traps" for a bouncing particle in which it stays for an average time τ . Let us furthermore assume that, after this time, the particle escapes just to the neighbouring trap to the left or to the right. Disregarding any correlations between subsequent jumps the random walk diffusion coefficient is given by

$$D_{rw}(f) = \frac{d^2}{2\tau(f)}; \quad (10)$$

where d is the distance between two wedges and τ is the escape time of a particle out of a wedge. For simple billiards such as Lorentz gases and related models this formula can be worked out exactly [9,8,35]. But here the dynamics is more complicated, hence we first obtain τ from computer simulations by restricting ourselves to frequency regions in which the dynamics is ergodic. The diffusion coefficient Eq. (10) resulting from this numerical input is shown in Fig.9.

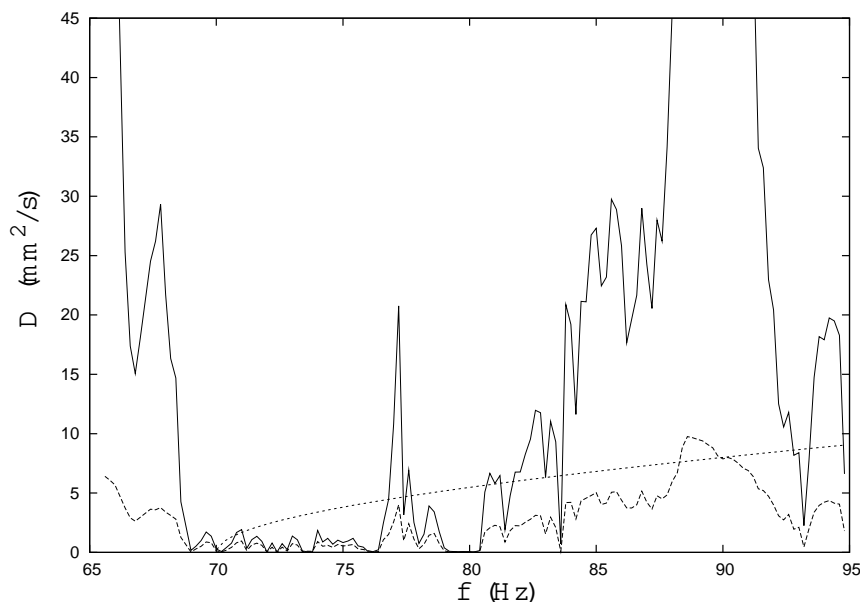


Fig. 9. Numerical and analytical evaluations of the random walk approximation Eq. (10) for the diffusion coefficient with frequencies $f > 65$ Hz. The bold line shows again the diffusion coefficient of Fig. 3, the dotted monotonously increasing curve represents the analytical formula Eq. (13), and the dashed irregular curve close to zero depicts Eq. (10) with the escape time computed numerically. The analytical approximation indicates some increase of the diffusion coefficient on coarse scales, whereas the numerical evaluation yields an irregular structure that is qualitatively very similar to the one of the precise diffusion coefficient.

The irregularities resulting from D_{rw} are qualitatively very close to the ones of the precise diffusion coefficient. This is easily understood by approximating the average escape time to

$$\left\langle \frac{d}{v_x} \right\rangle \approx \frac{d}{2E_x}; \quad (11)$$

hence the frequency dependence of the escape time must be very closely related to the frequency dependence of the horizontal kinetic energy E_x as shown in Fig. 5, whose functional form was already observed to be close to the one of the diffusion coefficient.

Eq. (11) furthermore provides a convenient starting point for a simple analyt-

ical approximation of the random walk diffusion coefficient Eq. (10). In order to find an analytical estimate for E_x we start from the energy balance

$$E = E_x + E_y + E_{\text{pot}} ; \quad (12)$$

where E is the average total energy and E_y gives the average vertical kinetic energy. $E_{\text{pot}} = gy$ is the average potential energy of the particle. We approximate the average height y with the amplitude of the vibrations, $y \approx A$, and the average total energy with the energy of the harmonic oscillator, $E \approx A^2 \omega^2 / 2$. The conjecture that the total energy of a moving particle is roughly proportional to ω^2 is also supported by a simplified version of a vibrating plate [36]. Finally, from computer simulations we approximate the relation between horizontal and vertical kinetic energy to $E_y \approx 19E_x$ reflecting the fact that only a small percentage of the energy vertically pumped into the system is transferred into the horizontal direction. This appears to be due to the very shallow geometry of the corrugated floor and to the action of the tangential friction. Taking all these expressions into account we get from Eq. (12) $2E_x \approx A^2 \omega^2 / 20 \approx gA = 10$. Inserting this expression into Eq. (11) and combining the resulting formula for D_a with Eq. (10) we get a simple analytical result for the random walk diffusion coefficient which is

$$D_a(f) \approx \frac{d^2}{2} \frac{1}{2E_x} \approx \frac{d^2}{2} \frac{A^2 \omega^2}{20} \frac{gA}{10} ; \quad (13)$$

This formula is depicted in Fig. 9. After a discontinuous, phase transition-like onset of diffusion it indicates some systematic but slow increase of the diffusion coefficient on a coarse scale. In the region of $f \in [80; 90]$ there is an analogy of this increase to the one obtained from the numerical evaluation of Eq. (10).

We now systematically refine the simple approximation Eq. (10) in order to further explore the origin of the irregular structure of the diffusion coefficient on fine scales. For this purpose we apply the scheme proposed in Ref. [8], which suggests to approximate the precise diffusion coefficient by adding higher-order terms to Eq. (10) according to a Green-Kubo formula for diffusion.

Let us still assume that a particle moves with a frequency of jumps $\omega = 1/\tau$ from traps to traps situated on a one-dimensional lattice at a distance d . Starting from the Einstein relation Eq. (9) one can prove that in the limit of infinitely many steps Eq. (9) is equal to the sum

$$D(f) = \frac{1}{\omega} \sum_{k=0}^{\infty} \langle x_k^2 \rangle - \langle x_0 \rangle^2 ; \quad (14)$$

which is a version of the Green-Kubo formula for an ensemble of particles

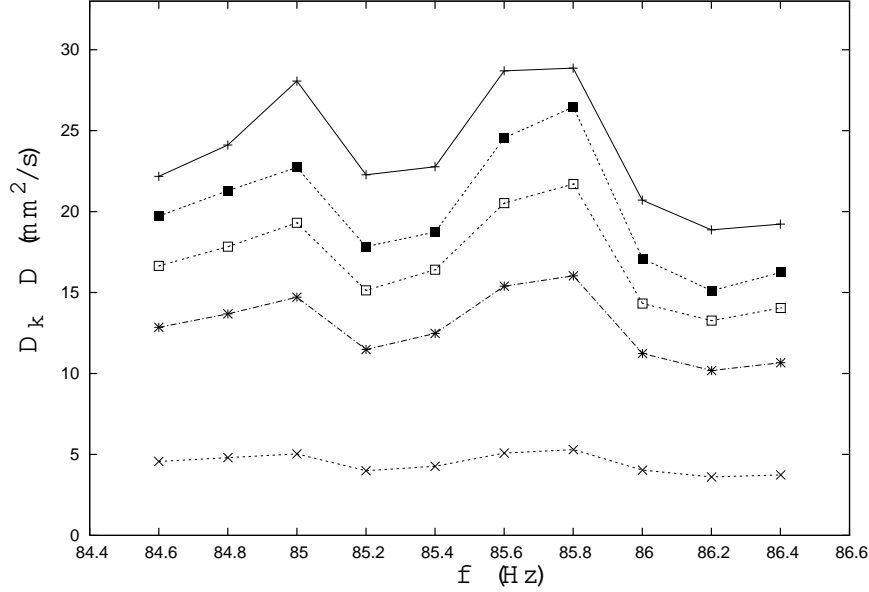


Fig. 10. Magnification of the frequency interval $f \in [84.6; 86.4]$ Hz in Fig. 3. The bold line on top shows the respective irregular diffusion coefficient on a fine scale, the lowest dotted line depicts the corresponding random walk approximation. The other lines represent a series of higher-order approximations refining this random walk and converging to this curve. These approximations $D_n(f)$ are obtained from the truncated Green-Kubo formula Eq. (15) for $n = 0; 2; 4$ and 7. The standard deviation errors are smaller than the magnitude of the symbols.

diffusing in a billiard [8]. Here $h(x_k)$ denotes jumps of a particle at position x_k at the k th time step in terms of respective lattice vectors, which here take the values $\pm d$. The first coefficient is $c_0 = 1/2$, and for $k > 0$ it is $c_k = 1$.

We now truncate this series after the n th time step yielding the systematic sequence of diffusion coefficient approximations

$$D_n(f) = \frac{d^2}{2} + \frac{1}{i\omega} \sum_{s_1 s_2 \dots s_n} p(s_1 s_2 \dots) h(s_1) h(s_2) \dots h(s_n) \quad (15)$$

Here $s_1 s_2 \dots$ denotes symbol sequences suitably identifying a particle's trajectory passing through the traps [8]. The averages in Eq. (14) are now given in terms of the conditional probabilities $p(s_1 s_2 \dots)$ that characterize all these possible trajectories. The first term in Eq. (15), that is, $D_0(f)$, is again the random walk approximation Eq. (10).

Let us now sketch of how to evaluate Eq. (15) to higher order. Let the first step be in the positive (right) direction with $h(x_0) = d$. The next jump is then defined by $h(x_1) = d_{s_1}$, where s_1 can be either f (forward) when the particle jumps to the right (in the same direction as the first one) or b (backward) when the particle jumps to the left, with $d_f = d$ and $d_b = -d$. If the dynam-

ics is deterministic and highly correlated, a particle starting from some tile may return to it with a probability that is different from the backscattering probability of a random walk, which is $1/2$. Hence, by feeding in the precise value for this probability as, e.g., computed from simulations one can suitably correct the random walk diffusion coefficient $D_0(f)$ in first order.

In detail, the first approximation $D_1(f)$ at time step 2 reads

$$D_1 = D_0 + 2D_0(p_f - p_b) = D_0 + 2D_0(1 - 2p_b) \quad (16)$$

depending on the backscattering probability p_b , respectively the forwardscattering probability p_f , only. In our case the value of p_f is considerably larger than the value of p_b , which is due to the fact that the height of the arcs of the circles between two traps is very shallow, thus yielding a considerable contribution to D_1 . In a similar way the second correction can be evaluated to

$$D_2 = D_1 + 2D_0(p_{ff} - p_{fb} + p_{bf} - p_{bb}) : \quad (17)$$

The probabilities associated to different symbol sequences were all computed numerically, and for the frequency interval of $f \in [84.6; 86.4]$ Hz the resulting approximations of increasingly higher order are shown in Fig. 10. Evidently, the random walk diffusion coefficient $D_0(f)$ is quantitatively much smaller than the numerically obtained value of the diffusion coefficient. However, by adding more and more terms representing repeated forward- and backward-scattering this series of approximations converges to $D(f)$. Note that in order to obtain a good approximation one has to go to relatively high order. That way, this figure exemplifies the impact of strong dynamical correlations on the diffusion coefficient. Furthermore, this convergence is obviously not monotonous in the frequency, with the higher order approximations revealing irregularities on fine scales. This behavior is well-known from related systems exhibiting deterministic diffusion [4, 11] and typically indicates the existence of a diffusion coefficient that is highly irregular as a function of the parameter, or possibly even fractal. The origin of these irregularities on finer scale may be attributed to the geometry of the scatterers, which make the system topologically unstable and induce a severe pruning of trajectories that is reflected in the diffusion coefficient. In other words, under parameter variation certain orbits may be forbidden, but the nature of forbidden orbits may change in a very intricate way [37].

In summary, we analyzed the frequency dependent diffusion coefficient on different scales: On a coarse scale and for large enough frequencies the diffusion coefficient appears to increase in qualitative agreement with a simple analytical random walk approximation. However, this behavior is largely suppressed by

a series of huge peaks that we attribute to the impact of resonances, which can be traced back to phase locking in the bouncing ball problem. Finally, successive evaluations of the Green-Kubo formula of diffusion give evidence for the existence of further irregularities on larger and larger scales that indicate higher-order dynamical correlations, and one may speculate that this curve is even of a fractal nature.

7 Conclusions

The purpose of this work was to analyze deterministic diffusion in a novel class of systems that we denoted as bouncing ball billiards. The geometry of this class of models is very similar to the one of some well-known chaotic Hamiltonian single-particle billiards such as Lorentz gases [1,2] in consisting of a periodic array of scatterers together with a point particle that collides with these obstacles. A particularly interesting case was studied in Ref. [10] composed of a periodically corrugated one-dimensional floor in which a particle experiences a constant vertical acceleration. Here evidence was given for the existence of a highly irregular, possibly fractal diffusion coefficient, as it was already found to exist in some very related, but somewhat simpler chaotic maps [4{6]. Our goal was to move this mechanical system closer to recent experiments on granular material, where similar geometries have been used. Hence, we made the collisions inelastic by introducing normal and tangential restitution coefficients. In this sense our model is somewhat related to the inelastic Lorentz gas of Ref. [38]. However, in order to compensate for this loss of energy at the collisions the surface was moving according to an oscillating driving force, just as it was done in respective experiments. Finally, we composed the periodic surface of circular scatterers that are very shallow. This way, our system is very close to the well-known problem of a ball bouncing inelastically on a flat surface, which is highly nonlinear and exhibits strong dynamical correlations in terms of phase locking. Hence, this setup enabled us to study features of chaotic diffusion in a specific granular one-particle system.

Our main numerical result is the existence of a highly irregular, possibly fractal diffusion coefficient as a function of the driving frequency. We performed a detailed analysis in order to understand the complicated structure of this curve and found that there are many different dynamical regimes depending on the driving frequency. The most pronounced effects are due to some previous regions of phase locking of the bouncing ball problem that still manifest themselves in form of huge peaks in the diffusion coefficient. Further features of our dynamics are parameter regions in which the particle's dynamics may "stick to" and "creep along" the surface. Although mostly associated to a very small value of the diffusion coefficient, this dynamics may also come together with a quasi-periodic orbit again exhibiting a huge peak at the position of a former

bouncing ball resonance. Finally, creeps and resonances may also coexist in form of some nonergodic dynamics evolving on two different attractors. We furthermore detected signs of a phase transition-like behavior at higher frequencies that, to some extent, seemed to match to a simple analytical random walk approximation. Refined approximations in form of correlated random walks, based on the systematic numerical evaluation of a Green-Kubo formula of diffusion, yielded evidence for the existence of further irregularities on finer and finer scales pointing towards a possible fractal structure of the frequency-dependent diffusion coefficient.

Due to the fact that both the bouncing ball and diffusion of granular particles on periodic surfaces are systems that have been profoundly studied in experiments [19,21-26], we hope that this paper stimulates further experimental work in order to verify this irregular frequency dependence of the diffusion coefficient. Of course we would not expect to reveal any fractal curve in a real experiment. However, we do believe that at least the largest peak is rather stable against random perturbations, as appears to be corroborated by the studies in Refs. [39,40]. Consequently, phenomena like the 1=1-resonance may show up in form of a local maximum of the diffusion coefficient as a function of the frequency. Again, we emphasize at this point that without further studies regarding the impact of perturbations on this billiard we cannot conclude to which extent dynamical correlations such as the ones reported in this paper may survive in case of a gas of interacting many particles. However, we note that in Refs. [20,41] the 1=1-phase locking regime of the bouncing ball was made responsible for the experimentally observed [20,42] phase transition between a quiescent amorphous and a gaseous state in a monolayer of a granular gas.

Of course, more theoretical work needs to be done in order to predict more details of possible experiments. There already exists an experimental setup measuring diffusion of single granular particles in one dimension [19], which is very close to our present model, however, the respective channels are presently asymmetric. On the other hand, computer simulations of a two-dimensional vibrating plate with circular scatterers would be close to the experimental device of Ref. [21]. Furthermore, of course there exist more realistic models for inelastic collisions than by using two constant restitution coefficients [34]. For example, one may wish to include the possibility of transfer of rotational energy of the moving particle at the collision.

One may also want to investigate the impact of a tilt on the bouncing ball billiard making it into a ratchet-like device. On the basis of our studies and related to the findings of Ref. [12], one may suspect that the current may exhibit again a highly irregular, possibly fractal structure as a function of control parameters reflecting the intrinsic properties of highly correlated chaotic transport. First signs of such irregularities indeed appear to be present in the

numerical and experimental data of Ref. [19]. It may also be elucidating to compute the spectrum of Lyapunov exponents and possibly other dynamical system's quantities, as well as time-dependent correlation functions and probability distributions of position and momentum variables for such types of bouncing ball billiards⁵ and to check their characteristics under parameter variation. Although simple reasoning suggests that the bouncing ball billiard is chaotic whenever there is a resonance, in form of providing at least one positive Lyapunov exponent, the features of the dynamical instability in parameter regions of stickiness is far from clear.

Another crucial point is to learn more about the dynamics of the standard bouncing ball problem with respect to the existence of higher-order resonances. As was shown in Ref. [29], for an approximate bouncing ball map in the limit of zero friction coefficient the complete set of tongues forms a very complicated fractal Devil's staircase-like structure in the parameter space. Unfortunately, for the general case up to now only the major Arnold tongues have been calculated, and to find more tongues, to adequately construct more details of the respective phase diagram, and to check in more detail for the existence of bifurcations in the inelastically bouncing ball problem appear to be open questions. However, in our case such information provided a roadmap in order to predict, and to understand, the irregular structure of the frequency-dependent diffusion coefficient, hence a respective analysis would be fundamental for further research along these lines.

Finally, we wish to remark that similar studies regarding the impact of phase locking on diffusive properties have been performed in Refs. [17,44]. However, in both cases the systems under investigation were very different from the granular model studied here: Ref. [17] outlined the impact of phase locking on the magnetoresistance in antidot-lattices under constant electric and magnetic fields and equipped with a bulk friction coefficient [17], whereas in Ref. [44] the authors analyzed the impact of phase locking on the diffusion coefficient for an overdamped stochastic Langevin equation with a ratchet-like asymmetric periodic potential under the influence of a periodic tilt force. The same Langevin equation, however, with a symmetric potential was used in Ref. [45] revealing again an enhancement of diffusion due to the matching of an average waiting time of a particle with the driving frequency. This nice paper as well as the very related studies of Ref. [46] point to a rather rich literature regarding the possible impact of stochastic resonance-like phenomena on the diffusion coefficient. Of course, the bouncing ball billiard too exhibits more important time scales, of which the average escape time is an example, hence we would

⁵ Note that periodic fine structures of probability distributions that are analogous to the ones reported in Ref. [43] were also detected in the chaotic maps of Ref. [5], hence we would conjecture that the bouncing ball billiard shows the same type of distributions representing basic features of deterministic dynamics.

indeed conjecture that there exist further resonances with the driving period in this model that may lead to additional modulations of the diffusion coefficient. To find such parameter regions further adds to the list of interesting open problems related to the bouncing ball billiard.

Acknowledgements

The authors wish to thank J. Urbach for making them aware of important literature regarding the bouncing ball problem. They are also grateful to him, to A. Prevost, to H.L. Swinney and to I. Janosi for remarks from the point of view of the granular material. Interesting discussion with A. Mehta and A. Pikovsky on synchronization and on the bouncing ball problem are gratefully acknowledged. Finally thanks H. Kantz for discussions on the construction of steady states, and T. Tel for critical remarks on the manuscript.

References

- [1] P. Gaspard, *Chaos, Shattering and Statistical Mechanics*, Cambridge University Press, Cambridge, England, (1998).
- [2] J.R. Dorfman, *An Introduction to Chaos on Nonequilibrium Statistical Mechanics*, Cambridge University Press, Cambridge (1999).
- [3] J. Vollmer, *Chaos, spatial extension, transport, and non-equilibrium thermodynamics*, *Phys. Rep.* 372, 131 (2002).
- [4] R. Klages and J.R. Dorfman, *Phys. Rev. Lett.* 74, 387 (1995).
- [5] R. Klages, *Deterministic Diffusion in One-Dimensional Chaotic Dynamical Systems*, Wissenschaft & Technik Verlag, Berlin (1996).
- [6] R. Klages, and J.R. Dorfman, *Phys. Rev. E* 59, 5361 (1999).
- [7] R. Klages and C. Dellago *J. Stat. Phys.* 101, 145 (2000).
- [8] R. Klages and N. Korabel *J. Phys. A*, 35, 4823 (2002).
- [9] T. Harayama, R. Klages, and P. Gaspard, *Phys. Rev. E* 66, 026211 (2002).
- [10] T. Harayama and P. Gaspard, *Phys. Rev. E* 64, 036215 (2001).
- [11] N. Korabel and R. Klages *Phys. Rev. Lett.* 89, 214102 (2002)
- [12] J. Groeneveld and R. Klages, *J. Stat. Phys.* 109, 821 (2002).
- [13] J.L. Lloyd, M. Niemeyer, L. Rondoni, and G.P. Morriss, *Chaos* 5, 536 (1995).

- [14] P. Gaspard and R. K. Lages, *Chaos* 8, 409 (1998).
- [15] D. Weiss et al., *Phys. Rev. Lett.* 66, 2790 (1991).
- [16] S. Weiss et al., *Europhys. Lett.* 51, 499 (2000).
- [17] J. Wiersig, K.-H. Ahn, *Phys. Rev. Lett.* 87, 026803 (2001).
- [18] K. J. Tanimoto, T. Kato, and K. Nakamura, *Phys. Rev. B* 66, 012507 (2002).
- [19] Z. Farkas, P. Tegzes, A. Vukics, and T. Vicsek, *Phys. Rev. E* 60, 7022 (1999).
- [20] W. Losert, D. G. W. Cooper, and J. P. Gollub *Phys. Rev. E*, 59, 5855 (1999).
- [21] A. Prevost, D. A. Egolf, and J. Urbach *Phys. Rev. Lett.* 89, 084301 (2002).
- [22] P. Pieranski, *J. Physique* 44, 573 (1983).
- [23] P. Pieranski, Z. J. Kovalik, and M. Franaszek, *J. Physique* 46, 681 (1985).
- [24] P. Pieranski and R. Bartolino, *J. Physique* 46, 687 (1985).
- [25] Z. J. Kovalik, M. Franaszek, and P. Pieranski, *Phys. Rev. A* 37 (1988) 4016.
- [26] N. B. Tullaro, T. Abbott and, J. Reilly, *An experimental approach to nonlinear dynamics and chaos*, Addison Wesley Publ., New York (1992).
- [27] J. Guckenheimer and P. Holmes *Nonlinear Oscillations, Dynamical Systems and Bifurcations of Vector Fields*, Springer, New York, 5th edition (1997).
- [28] A. Lichtenberg and M. Leiberman, *Regular and Stochastic Motion*, Springer, New York (1983).
- [29] A. M. Luchta and J. M. Luck, *Phys. Rev. Lett.* 65, 393 (1990).
- [30] J. M. Luck and A. M. Luchta, *Phys. Rev. E* 48, 3988 (1993).
- [31] U. Feudel, C. Grebogi, B. R. Hunt, and J. A. Yorke, *Phys. Rev. E* 54, 71 (1996).
- [32] P. Devillard, *J. Phys. I* 4, 1003 (1994).
- [33] P. Gaspard, *Phys. Rev. E* 53, 4379 (1996).
- [34] S. M. Foerster, M. Y. Louge, H. Chang, and K. Allia, *Phys. Fluids* 6, 1108 (1994).
- [35] J. M. Luchta and R. Zwanzig, *Phys. Rev. Lett.* 50, 1959 (1983).
- [36] S. Warr and J. M. Huntley, *Phys. Rev. E* 52, 5596 (1995).
- [37] P. Cvitanovic, R. Artuso, R. Mainieri, G. Tanner and G. Vattay, *Classical and Quantum Chaos*, www.nbi.dk/ChaosBook/, Niels Bohr Institute (Copenhagen 2001)
- [38] R. K. Lages, K. Rateitschak and G. Nicolis, *Phys. Rev. Lett.* 84 4268 (2002).
- [39] R. K. Lages, *Phys. Rev. E* 65, 055203(R) (2002).

- [40] R. Klages, *Europhys. Lett.* 57, 796 (2002).
- [41] X. Nie, E. Ben-Naim and S.Y. Chen, *Europhys. Lett.* 51, 679 (2000).
- [42] J.S. Olsen and J.S. Urbach, *Phys. Rev. Lett.* 98, 4369 (1998).
- [43] S. Warr, W. Cooke, R. C. Ball, and J.M. Huntley, *Physica A* 231, 551 (1996).
- [44] D. Reguera, P. Reinann, P. Hanggi and J.M. Rubi *Europhys. Lett.* 57, 644 (2002).
- [45] M. Schreier, P. Reinann, P. Hanggi and E. Pollak *Europhys. Lett.* 44, 416 (1998).
- [46] P. Fulde, L. Pietronero, W. R. Schneider, and R. Strassler, *Phys. Rev. Lett.* 35, 1776 (1975).